IJFANS INTERNATIONAL JOURNAL OF FOOD AND NUTRITIONAL SCIENCES
ISSN PRINT 2319 1775 Online 2320 7876

Research paper UGC CARE Listed (Group -I) Journal Volume 11, Iss 12, Dec 2022

Mathematical Modeling for EVS Prediction on Inverter Switching Functions: Assessment on Four Switch BLDC Motor Drive

[1]Dr.V.Anil Kumar, [2]T. Srikanth, [3]Dr.G.Madusudhana Rao, [4]Dr. C.Nithyanandam
[1,2,3,4]Dept of Electrical and Electronics Engineering, Sree Venkateswara College Of Engineering, Nellore (Dt), Andhra Pradesh, India.

ABSTRACT
As the present study, switching functions can be used to mimic a Four-Switch, Three-Phase Inverter (FSTPID) Brushless DC (BLDC) motor drive. The recommended representation shows the drive steady state and transient performance using inverter switching functions rather than actual circuits. The power conversion system, the BLDC motor, and the current and speed control system are all researched as part of the overall BLDC motor drive investigation. The tools Matlab/Simulink are used to implement the precise and approachable proposed model. This concept may be applied to demonstrate particular electrical variables, including phase current, line and phase voltages, diode and switch currents. Because issues occurred when two power switches were removed, direct phase current (DPC) control is utilized. Simulations and experimentation are used to verify the model that has been suggested.
Keywords: modeling, simulation, brushless DC motors, DSP, switching function

1. INTRODUCTION

Due to its higher power density and simplicity of production, brushless DC (BLDC) motors are employed in automotive and domestic employ. Reduced BLDC motor drive manufacturing costs are also crucial for some applications [1]. BLDC motor drives can be made more affordable by deleting the sensors and lowering the amount of power switches [2]. Predicting the presentation of an electric motor is crucial in order to analyze the characteristics of motor designs and motor modelling. Instead of developing motor prototypes, which takes more time and money, simulation design is advised for creating motors [3]. Software for simulating electronic circuits and dynamic systems falls into two categories: (1) Software for modelling circuits, such as PSPIDce (2) software for solving equations, like as Matlab. Users must create their own models to meet their demands because these programmers were not created expressly for power electronic systems [4]. The entire four-switch BLDC motor drive is modelled in this study using the well-known functional switching-based modelling approach, which is implemented in Simulink software.

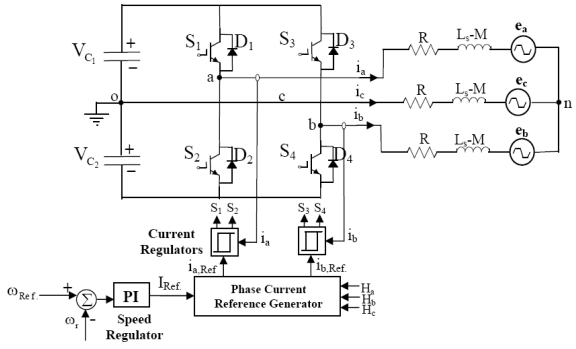

Figure 1 demonstration of a three-phase, four-switch inverter BLDC motor utilizing the DPC control method.

Fig. 2 displays the results of the position Hall Effect sensor, the current wave forms, and the trapezoidal

Research paper UGC CARE Listed (Group -I) Journal Volume 11, Iss 12, Dec 2022

back-EMF wave forms of a three-phase BLDC motor. To provide the motor using the most constant torque possible, phase currents and corresponding phase back-EMF voltages must be coordinated. Additionally, depending on the mode, only two phases are active at once, and the final phase is ineffective. On the other hand, a four-switch inverter's constrained voltage vectors make it impossible to generate wave forms with 120 conducting current [2]. A three-phase BLDC motor is operated using the four-switch inverter architecture and the Direct Phase Current (DPC) management technique created by B.K. Lee [2]. This technique allows independent management of phase A and phase B currents in phases 2 and 5. As can be seen in Fig. 3, the back-EMF voltage of phase C does not obstruct the phase electrical currents.Table 1 summaries the command patterns off our-switch inverter for every mode.

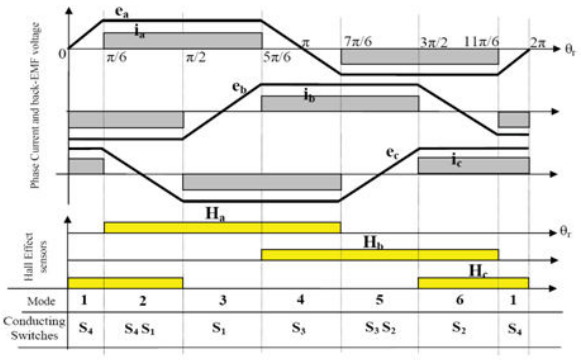

Fig.2 – Phase back-EMF, current and position Hall effect sensors wave form so fathree-phase BLDC Moto

Hall Sensors	Modes	Active Phases	Silent Phase	Switched Devices
100	Mode 1	B,C	A	S4
101	Mode 2	A,B	C	S1,S4
001	Mode 3	A,C	B	S1
011	Mode 4	B,C	A	S3
010	Mode 5	A,B	C	S2,S3
110	Mode 6	A,C	B	S2

Table1.Switching sequence of FSTPID-BLDC

II. MODEL OF FSTPID-BLDC MOTOR DRIVE DEPENDING ON SWITCHING UTILITY PERCEPTION

Perceptive and improving the execution of static power inverters can be done by exploitation switching function idea [6]. Power conversion circuits is shapely by means of switching functions instead of circuit typologies to better reflect their functions [7]. The total power conversion functions can be simplified as a result, and it also makes it possible to establish analytical concepts that apply to converter families rather than single converters [8]. PsPIDce is able to used to apply the switching function notion, albeit incorporating the circuit components lengthens simulation time. The representation is then swiftly constructed using Simulink's functional building components. The suggested layout is shown as a schematic diagram in Fig. 4 for a three-phase, four-switch inverter BLDC motor drive. It consists of the following five functional building blocks: a BLDC motor, a current controller, a power inverter, an acceleration controller, and a switch-diode present calculator.

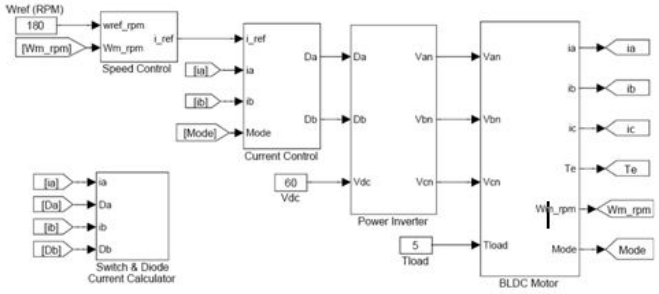

Fig. 4 – The complete block diagram of the switching function idea modelling of a four-switch BLDC motor drive

BLDC Motor Block

The two inputs for this component are the load's torque and the terminals that contain phase voltages. The backEMF generator, present calculation, torque computation, and position and speed assessment are the four components which make up this block. The BLDC motor block is displayed in Fig. 5. Back-EMF is a function of rotor position (r) and possesses an intensity of E=Kem, wherein m is the rotor's mechanical velocity and Ke is the back-EMF constants.. The back-EMF of phase might vary depending on the rotor position A, for instance, can be stated as follows: () () () + = 6E / 12E 11 / 6 2 E 7 / 6 11 / 6 6E (2) Lock-up table methods in Simulink can be used to implement back-EMF phase voltage.

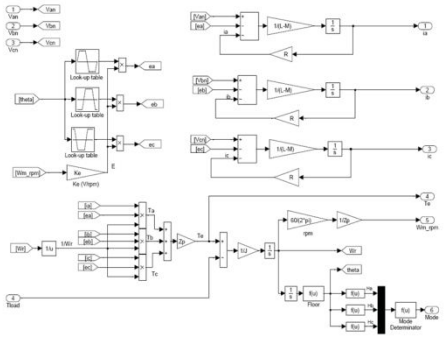

Fig. 5 - Simulink execution of the BLDC motor block

The differential equations (1) is revised to the following to obtain the phase currents:

$$\begin{cases} \frac{di_a}{dt} = \frac{1}{L_s - M}\left(v_{an} - e_a - R \cdot i_a\right) \\ \frac{di_b}{dt} = \frac{1}{L_s - M}\left(v_{bn} - e_b - R \cdot i_b\right) \\ \frac{di_c}{dt} = \frac{1}{L_s - M}\left(v_{cn} - e_c - R \cdot i_c\right) \end{cases}$$

Therefore, the electromagnetic torque (Te) is obtained from

$$T_e = \frac{Z_p}{2 \cdot \omega_r}\left(e_a i_a + e_b i_b + e_c i_c\right)$$

B. Current Control Block

A traditional controller like a PID or hysteresis controller can be taken into consideration for current regulation. The quick dynamic responses during transient phases are obtained in this research using bipolar hysteresis current control. Only phase A of the current control strategy is explained. The active switches or diodes used to control phase A current are shown in Fig. 6. This hysteresis band is indicated by the maximum and lower limits of the phase current, that are set to 1.05 and 0.95, correspondingly. According to Fig. 7, the current control block carries out the hysteresis current control logic. utilizing the appropriate

Research paper UGC CARE Listed (Group -I) Journal Volume 11, Iss 12, Dec 2022

Matlab functions (f(u)), the current control block creates the two switching equations Da and Db as follows utilizing the determined phase currents (ia, ib), the current reference (i_ref), and the operational method: two switchable features, Da and Db, are produced like the following using the appropriate Matlab functions (f(u)) and operating mode:

Moreover, the terminal voltages vao and vbo are obtained as:

$$D_a = ((u[4]==2)+(u[4]==3))\cdot\begin{bmatrix}(u[1]<u[3]*0.95)-(u[1]>u[3]*1.05)+\\(u[1]>u[3]*0.95)*(u[1]<u[3]*1.05)*(u[1]>u[2])-\\(u[1]>u[3]*0.95)*(u[1]<u[3]*1.05)*(u[1]<u[2])\end{bmatrix}$$
$$+((u[4]==5)+(u[4]==6))\cdot\begin{bmatrix}-(u[1]>-u[3]*0.95)+(u[1]<u[3]*1.05)-\\(u[1]<-u[3]*0.95)*(u[1]>-u[3]*1.05)*(u[1]<u[2])+\\(u[1]<-u[3]*0.95)*(u[1]>-u[3]*1.05)*(u[1]>u[2])\end{bmatrix} \quad (9)$$

$$D_a = ((u[4]==4)+(u[4]==5))\cdot\begin{bmatrix}(u[1]<u[3]*0.95)-(u[1]>u[3]*1.05)+\\(u[1]>u[3]*0.95)*(u[1]<u[3]*1.05)*(u[1]>u[2])-\\(u[1]>u[3]*0.95)*(u[1]<u[3]*1.05)*(u[1]<u[2])\end{bmatrix}$$
$$+((u[4]==1)+(u[4]==2))\cdot\begin{bmatrix}-(u[1]>-u[3]*0.95)+(u[1]<u[3]*1.05)-\\(u[1]<-u[3]*0.95)*(u[1]>-u[3]*1.05)*(u[1]<u[2])+\\(u[1]<-u[3]*0.95)*(u[1]>-u[3]*1.05)*(u[1]>u[2])\end{bmatrix} \quad (10)$$

$$\begin{cases} V_{ao} = \dfrac{V_{dc}}{2}\cdot D_a \\ V_{bo} = \dfrac{V_{dc}}{2}\cdot D_b \end{cases}$$

that V_{dc} is the voltage across of DC-bus.

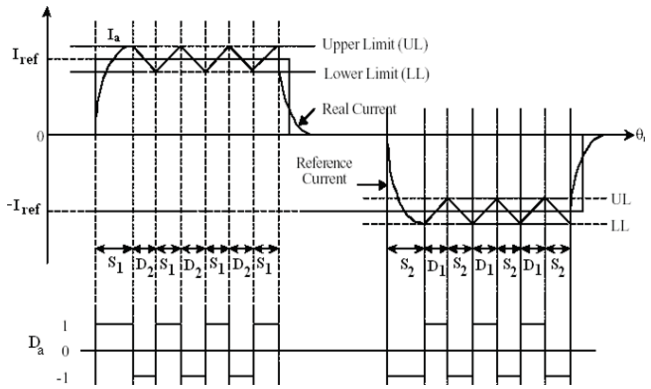

Fig. 6 – Hysteresis current control of phase A

Research paper UGC CARE Listed (Group -I) Journal Volume 11, Iss 12, Dec 2022

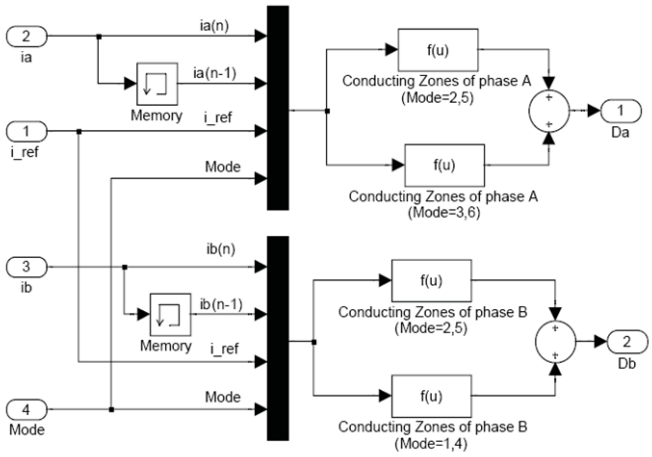

Fig. 7 – Direct phase current (DPC) regulation of the Current Control block in Simulink

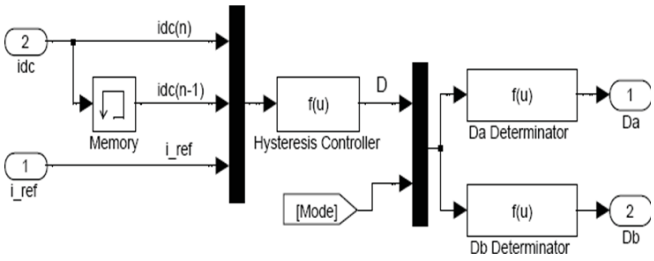

Fig. 8 – Current Control block execution in Simulink utilizing DC-Link current regulation

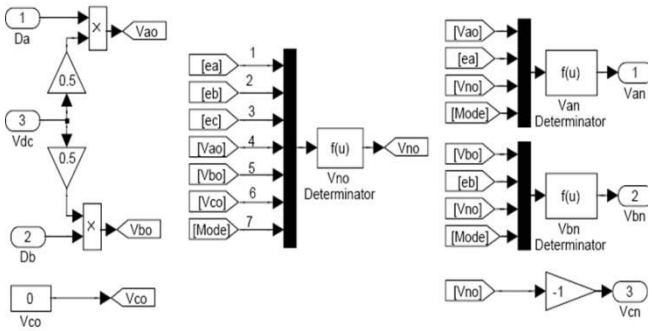

Fig.9

c. Speed Control Block

As depicted in Fig. 10, this collection uses a PID controller to control the rotor speed. In the current control block, it generates the current reference. The motor torque is thus immediately controlled by altering the present-day reference displacement as:

$T_{ref} \square K_t \square i_{ref}$

where Kt is torque steady and Iref is acknowledgment current.

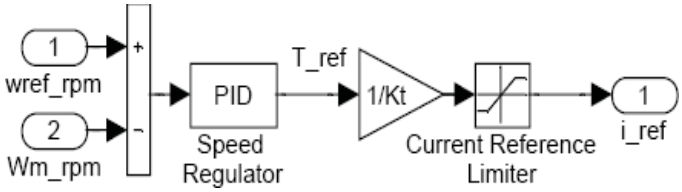

Fig. 10 – execution of Speed Control block

D. Switch and Diode Current calculator Block

Applying the switching equations Da and Db, exact pure switch and diode currents are determined from the estimated phase currents. A value that is positive of Dx (x=a,b) suggests the top switch of the

Research paper UGC CARE Listed (Group -I) Journal Volume 11, Iss 12, Dec 2022

relevant phase conducts when the phase current is controlled at a positive level, whereas a negative value of Dx implies that the bottom diode is flowing. For negative present values, the reverse rule applies. Fig. 11 depicts how this block is implemented in Simulink. Switch and diode duty cycles are determined by:

$$\begin{cases} D_{a\_S1} = (i_a > 0)\cdot(D_a > 0) \\ D_{a\_D2} = (i_a > 0)\cdot(D_a < 0) \\ D_{a\_S2} = (i_a < 0)\cdot(D_a < 0) \\ D_{a\_D1} = (i_a < 0)\cdot(D_a > 0) \end{cases} \begin{cases} D_{b\_S3} = (i_b > 0)\cdot(D_b > 0) \\ D_{b\_D4} = (i_b > 0)\cdot(D_b < 0) \\ D_{b\_S4} = (i_b < 0)\cdot(D_b < 0) \\ D_{b\_D3} = (i_b < 0)\cdot(D_b > 0) \end{cases} \quad (19)$$

Therefore the currents of switches, diodes and DC-bus

Thus, to determine the currents of switches, diodes, and DC-bus capacitors:

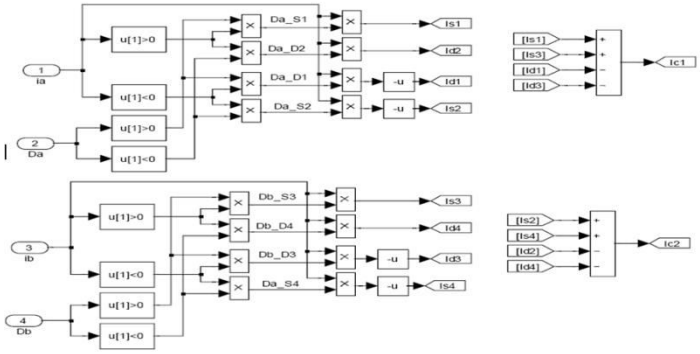

Fig. 11 – Control and Diode Current Calculating machine block

3. SIMULATION

Table2 summarizes the specifications of the employed BLDC motor. This motor has a low speed and great torque for use in bicycles. There is a 5 [N.m] load torque, 180 [rpm] reference speed, and 60 [V] DC-bus voltage. Initially the capacity of a four-switch inverter's DPC control technique is contrasted with that of a six-switch inverter's regulation of current and a four-switch inverter's DC-link current control approach. The simulation of every approach is presented in Fig. 12. The rectangular current wave forms result from the DPC control system outperforming even a six-switch inverter. Yet, the DC-link current control strategy has issues because of the effect of voltage ec in modes 2 and 5. The phase current wave forms in commutation may be shown using modelling that utilities the concept of switching functions. The present shift from phase A to phase B is illustrated in Fig. 13. As a result of the potential that currents ia and ib cannot exceed the reference ideals simultaneously, the behaviour of freewheeling diodes. As a result, phase C current has ripple, which causes commutation torque ripple [9]. Movement consequence at 180 [rpm] of speed reference

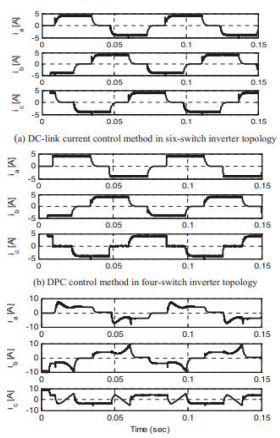

depicted in Fig. 14. The rotor speed reaches the reference speed in 0.01 seconds. [Sec].

Fig. 12 A comparison of the DC-link current control technique and the DPC approach in four- and six-switch inverters operating at 100 rpm

Research paper UGC CARE Listed (Group -I) Journal Volume 11, Iss 12, Dec 2022

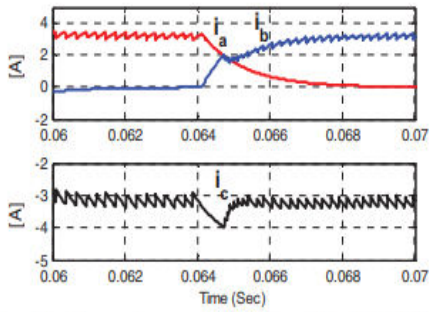

Fig. 13 – Current commutation from A to B at 100 rpm

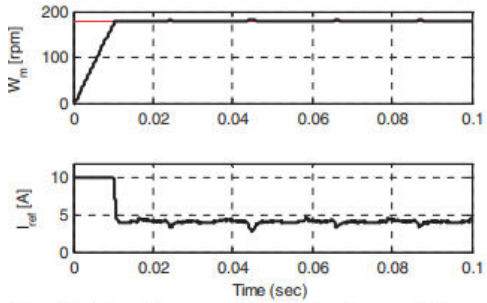

Fig. 14 – Speed response to speed reference 180 rpm

Fig. 15 displays immediate and RMS waveforms of the paragraph-to-line, terminal, and motor star point voltages at regard to o (the centre of the DC-bus) at an acceleration of 180 [rpm]. The essential variables utilised by this modelling technique, Da and Db, are also shown in Fig. 15 as the switching function. Modes 2 and 5 have higher switching frequencies compared to other modes due to increased DC voltage across the switches. Efficiency of the inverter in mode 5 is depicted in Fig. 16. Considering that they originate from separate current regulators, the switching commands to switches S3 and S2 are distinct.

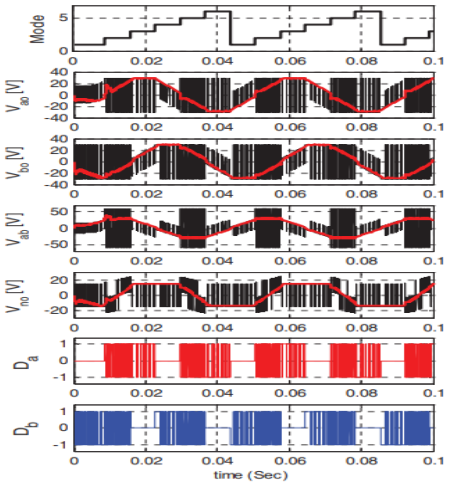

Fig.15 Line-

toline voltages and switching functions Da and Db at 180 rpm, in terms of instantaneous and RMS values.

Research paper UGC CARE Listed (Group -I) Journal Volume 11, Iss 12, Dec 2022

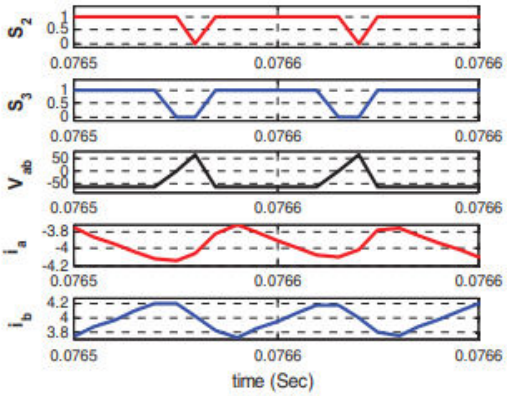

Fig. 16 – Switching of the inverter in mode 5

3.1 Execution

Fig. 17 demonstrates the experimental set-up. A DSP controller, model number TMS320LF2407A, is used to control the entire system. Without employing the direct phase current (DPC) control method, the phase current waveforms are demonstrated in Fig. 18. It is clear that the back-EMF voltage of phase C influences phase B and phase C currents. The simulated results in Fig. 12 are supported by experimental data. Fig. 19 displays the signals for four switches. For instance, in mode 2, the commands for S1 and S4 are the same. The rectangular phase current waveforms are finally achieved utilising the DPC control technique and are displayed in Fig. 20. In Fig. 21, equivalent switching signals are displayed. These graphs support the simulation findings in Figs. 12 and 16.

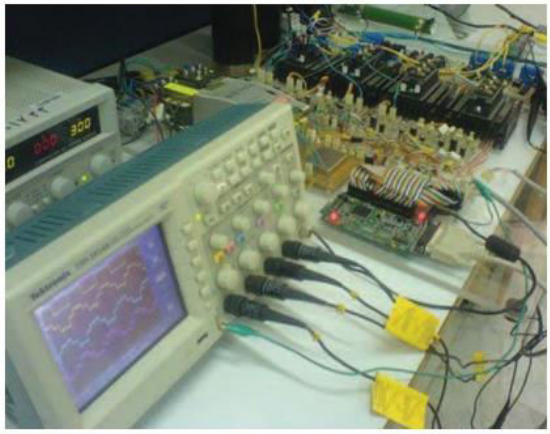

Fig. 17 – investigate setup of BLDC motor drive system

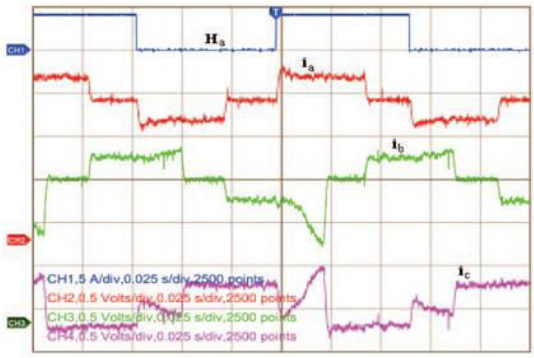

Fig. 18 – Hall sensor Ha and phase current wave forms with no exploitation the DPC control performing (IDC control technique)

Research paper UGC CARE Listed (Group -I) Journal Volume 11, Iss 12, Dec 2022

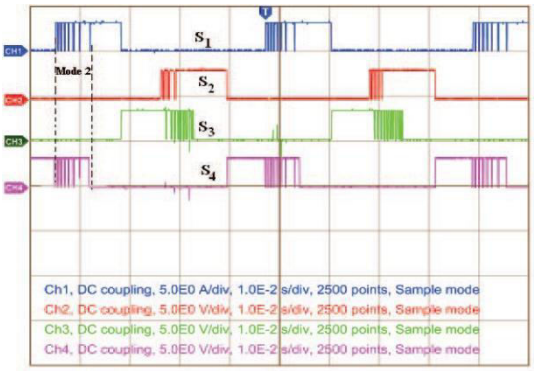

Fig. 19 – Without using the DPC control mechanism, command signals are sent to the switches.

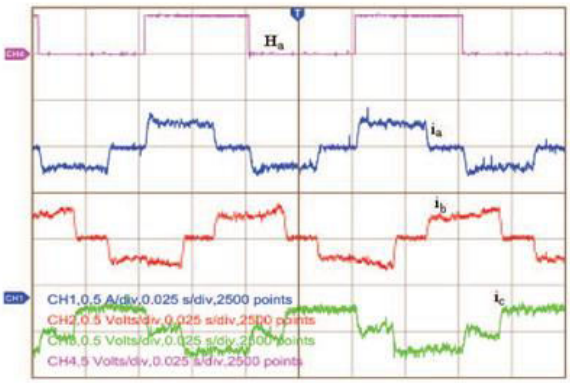

Fig. 20 – Hall sensor Ha and phase current waveforms while employing the DPC control method

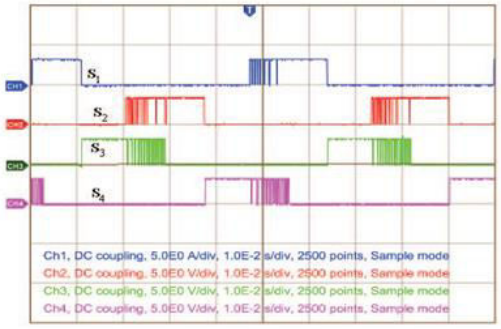

Fig.21.When using the DPC control method, command signals are sent to the Power Switches.

CONCLUSION

This work investigates the impulsive system of a BLDC motor drive with fewer switches, that is applied in inexpensive applications. Using a useful model, a four-switch inverter BLDC motor drive has been created depending on the switching functions concept (SFC) due to the importance of evaluating an electrical drive's performance prior to considering manufacturing issues. The following are the main advantages of the SFC-based model: circuitry for power conversion that is simpler offering a user-friendly design tool

Extensible Simulation has been utilized to demonstrate the validity of the suggested model because of its modular construction. By taking into account non-ideal back-EMF voltage wave forms, commutation torque ripple, and other factors, the execution of the suggested drive is developed. A DSP-based experimental set up has been constructed to confirm the simulation and analysis results. A TMS320F2407Achip serves as the drive system's control core. Finally, it has been demonstrated that the urbanized representation and the

recreation consequences are supported by the experimental results.

REFERENCES

1. P. PIDllay, R. Krishnan; "Analysis of permanent-magnet motor drives. I: The permanent-magnet synchronous Motor Drive",IEEE Transactions on Industry Applications, vol. 25, No. 2,March1989,pp.265-273.
2. B.K. Lee, T.H. Kim, M. Ehsani; "On the feasibility of four-switchthree-phaseBLDCmotordrivesforlowcostcommercialapplications:topologyandcontrol",IEEETransactions on Power Electronics, Vol. 18, No. 1, pp. 164-172,January2003.
3. P. PIDllay, R. Krishnan; "Modeling, simulation, and analysis ofpermanent-magnet motor drives. II: The Brushless DC MotorDrive", IEEE Transactions on Industry Applications, vol. 25,No.2,March/April1989,pp.274-279.
4. C.K. Lee and M. Ehsani; "A simplified functional model for3-phasevoltage-sourceinverterusingswitchingfunctionconcept", in Conf.Rec. IEEE-IECON, pp.462-467, 1999.
5. A.HalvaeiNiasar, H. Moghbeli, A. Vahedi; "Modeling andSimulationMethodsforBrushlessDCMotorDrives",Proceeding of the First International Conference on Modeling,Simulation and Applied Optimization (ICMSAO'05), pp.05-6/05-6, February2005,Sharjah,U.A.E.
6. B.K. Lee and M. Ehsani; "Advanced BLDC Motor Drive forLowCostandHighPerformancePropulsionSysteminElectricandHybridVehicles",2001IEEEInternationalElectric Machines and Drives Conference, 2001, Cambridge,MA,June2001,pp.246-251.
7. L.Salazar,G.Joos;"PSPIDCESimulationofThree-Phaseinverters by Means of switching Functions", IEEE Trans. OnPower Electronics,Vol.9,No.1,pp.35-42January1994.
8. E.P.Wiechmann,P.D.Ziogas,V.R.Stefanovic;"GeneralizedFunctionalModelforThreePhasePWMInverter/Rectifier Converters", in Proc. IEEE IAS'85, 1985,pp.984-993.
9. A.HalvaeiNiasar, A. Vahedi, H. Moghbelli; "Analysis and Control of Commutation Torque Ripple in Four-Switch,Three-Phase Brushless DC Motor Drive", Proceeding of the 2006 IEEE International Conference on Industrial Technolog y(ICIT06),pp.239-246, India.